J|A|C|S ARTICLES

Published on Web 08/12/2009

Mechanism and Transition State Structure of Aryl Methylphosphonate Esters Doubly Coordinated to a Dinuclear Cobalt(III) Center

Guoqiang Feng,[†] Eric A. Tanifum,[‡] Harry Adams,[†] Alvan C. Hengge,*[,‡] and Nicholas H. Williams*[,†]

Utah State University, Department of Chemistry and Biochemistry, Logan Utah 84322-0300, and University of Sheffield, Centre for Chemical Biology, Department of Chemistry, Sheffield, UK S3 7HF

Received May 21, 2009; E-mail: alvan.hengge@usu.edu; N.H.Williams@Sheffield.ac.uk

Abstract: Reactivities of five phosphonate esters each coordinated to a dinuclear Co(III) complex were investigated ($[Co_2(tacn)_2(OH)_2\{O_2P(Me)OAr\}]^{3+}$; tacn = 1,4,7-triazacyclononane; substituent = *m*-F, *p*-NO_2 (**1a**); *p*-NO_2 (**1b**); *m*-NO_2 (**1c**); *p*-Cl (**1d**); unsubstituted (**1e**)). Hydrolysis of the phosphonate esters in **1a** to **1e** is specific base catalyzed and takes place by intramolecular oxide attack on the bridging phosphonate. These data define a Brønsted β_{lg} of −1.12, considerably more negative than that of the hydrolysis of the uncomplexed phosphonates (−0.69). For **1b**, the kinetic isotope effects in the leaving group are $^{18}k_{lg}$ = 1.0228 and ^{15}k = 1.0014, at the nonbridging phosphoryl oxygens $^{18}k_{nonbridge}$ = 0.9954, and at the nucleophilic oxygen $^{18}k_{nuc}$ = 1.0105. The KIEs and the β_{lg} data point to a transition state for the alkaline hydrolysis of **1b** that is similar to that of a phosphate monoester complex with the same leaving group, rather than the isoelectronic diester complex. The data from these model systems parallel the observation that in protein phosphatase-1, which has an active site that resembles the structures of these complexes, the catalyzed hydrolysis of aryl methylphosphonates and aryl phosphates are much more similar to one another than the uncomplexed hydrolysis reactions of the two substrates.

Introduction

Phosphate esters abound in nature and play critical roles in key biological processes such as cell growth, proliferation and differentiation, metabolism, cell signaling, and gene expression. Phosphonate esters, on the other hand, are not as widely distributed in nature[1] and their natural role in biological systems is still being unraveled. However, the potential of phosphonates as phosphate mimics in biological systems has been well established.[2] Several phosphonic acid derivatives, both natural and synthetic, are widely used in medicine and agriculture.[1,3] In previous studies, carried out mostly on neutral phosphonate esters (phosphate triester analogs), hydrolysis catalyzed by amines was found to follow general base catalysis with P−O bond formation significant in the transition state.[4] To the best of our knowledge, limited mechanistic studies have been carried out on the hydrolysis of phosphonate ester monoanions (phosphate diester analogs). The most detailed study involved the analysis of phenyl methylphosphonate and 4-nitrophenyl methylphosphonate by Edwards et al..[5] The hydrolysis of both compounds involves base catalyzed and spontaneous components, and small effects from added cations (Ba(II) and Ca(II)). Tsubouchi and Bruice have used methylphosphonates as analogues for phosphate diesters in studying the effect of La ions on the cleavage reaction,[6] and Lönnberg et al. have used phosphonates as noncleavable analogues of RNA to study isomerization of phosphoryl groups between the 2′ and 3′ positions of ribose rings.[7] In both cases, comparable reactivity and similar mechanistic pathways to the diester was observed or inferred. Kinetic isotope effects (KIE) along with activation parameters and linear free energy relationships (LFER) studies will provide different but complementary data, which together can give a detailed characterization of transition state structures and mechanisms of such reactions.

The hydrolysis of phosphate esters in biological systems is mediated by phosphatases. Most phosphatases are specific to the degree of esterification of the substrate, but some have

[†] University of Sheffield.
[‡] Utah State University.

(1) Quin, L. D. In *A Guide to Organophosphorus Chemistry*; John Wiley & Sons: New York, 2000; pp 357−386.
(2) Engel, R. *Chem. Rev.* **1977**, *77*, 349–367.
(3) Hilderbrand, R. L. In *The role of phosphonates in living systems*; CRC Press: Boca Raton, FL, 1983; pp 97−104; Hori, T.; Horiguchi, M.; Hayashi, A. *Biochemistry of natural C-P compounds*; Japanese Association for Research on the Biosynthesis of C-P Compounds: Maruzen, Kyoto, Japan, 1984.
(4) Kovach, I. M.; Bennet, A. J.; Bibbs, J. A.; Zhao, Q. J. *J. Am. Chem. Soc.* **1993**, *115*, 5138–5144. Brass, H. J.; Bender, M. L. *J. Am. Chem. Soc.* **1972**, *94*, 7421–7428.
(5) Behrm, E. J.; Biallas, M. J.; Brass, H. J.; Edwards, J. O.; Isaks, M. *J. Org. Chem.* **1970**, *35*, 3063–3069. Behrman, E. J.; Biallas, M. J.; Brass, H. J.; Edwards, J. O.; Isaks, M. *J. Org. Chem.* **1970**, *35*, 3069–3075.
(6) Tsubouchi, A.; Bruice, T. C. *J. Am. Chem. Soc.* **1994**, *116*, 11614–11615. Tsubouchi, A.; Bruice, T. C. *J. Am. Chem. Soc.* **1995**, *117*, 7399–7411.
(7) Lonnberg, T.; Kralikova, S.; Rosenberg, I.; Lonnberg, H. *Collect. Czech. Chem. Commun.* **2006**, *71*, 859–870. Maki, E.; Oivanen, M.; Poijarvi, P.; Lonnberg, H. *J. Chem. Soc., Perkin Trans. 2* **1999**, 2493–2499. Oivanen, M.; Mikhailov, S. N.; Padyukova, N. S.; Lonnberg, H. *J. Org. Chem.* **1993**, *58*, 1617–1619.

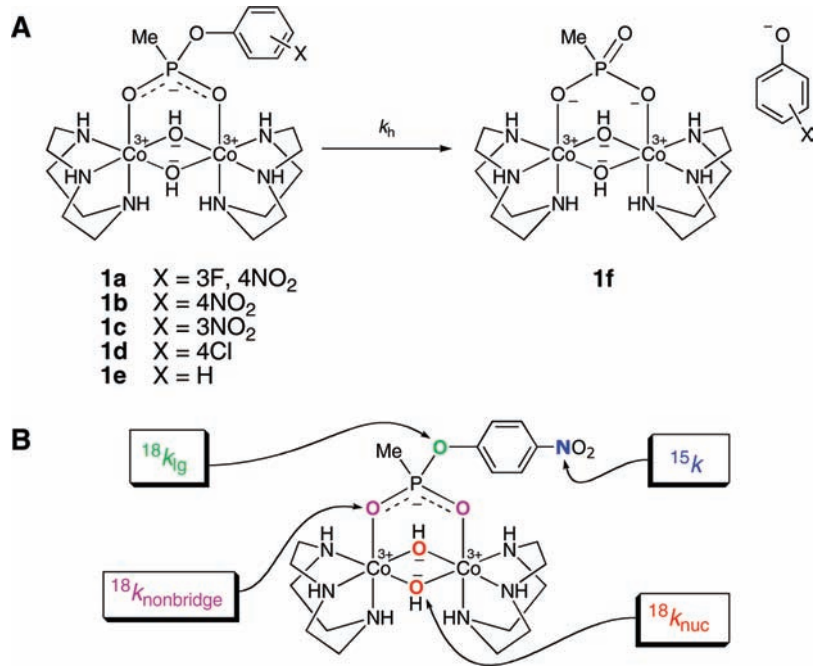

Figure 1. (A) Reaction scheme for kinetic studies on the hydrolysis of TACN-Co(III) complex-bound aryl methylphosphonates. (B) Positions of kinetic isotope effect measurements in complex **1b**.

evolved to catalyze the hydrolysis of both phosphate mono- and diester substrates. Others such as 5′-nucleotide phosphodiesterase,[8] acid (histidine) phosphatase,[9] and protein phosphatase-1 (PP1)[10] can catalyze the hydrolysis of phosphonate esters as well. While there is considerable literature data concerning the characterization of enzyme-catalyzed, model complex-catalyzed, and uncatalyzed mechanisms and transition state structures of phosphate ester hydrolysis, little data is available for phosphonate esters.

The phosphoprotein phosphatases constitute a family characterized by very similar active sites containing a binuclear metal center in which the metal ions are separated by ~3 Å. Although the exact mechanism is not well understood, they have been proposed to activate a water molecule for direct hydrolysis of the phosphate ester bond. Simple dinuclear metal complex models such as **1**, capable of reproducing structural and functional properties of protein phosphatases, can give insights into their catalytic mechanisms and transition state structures. The metal−metal distance in **1** (2.9 Å), is comparable to those found in kidney bean purple acid phosphatase (KBPAP) (3.1 Å)[11] and PP1 (3.3 Å).[12] Complex **1** accelerates the rates of hydrolysis of bound aryl phosphate monoesters by about 10^{11} fold[14] and diesters by about 10^{10}-fold.[15] [Note: As the reaction of the monoester dianion is pH-independent in this region, whereas the reaction of the complex is specific base catalyzed, only a simple comparison of the rates under the same conditions can be made directly. The pseudo first-order rate constant for the hydrolysis of 4-nitrophenyl phosphate in 0.5 M NaOH at 25 °C is about 2×10^{-9} s^{-1} (extrapolated from published data).[13] Under the same conditions, 4-nitrophenyl phosphate coordinated to **1** has a pseudo first-order rate constant of 200 s^{-1}, representing a 10^{11}-fold rate acceleration for phosphate monoester hydrolysis. If an upper limit for the rate constant for specific base catalyzed hydrolysis of the monoester dianion in solution ($<4 \times 10^{-10}$ M^{-1} s^{-1} if less than 10% of the reaction follows this pathway in 0.5 M NaOH) is used for this comparison, the rate acceleration would be even higher ($>10^{12}$).] KIE studies on *p*-nitrophenyl phosphate and methyl *p*-nitrophenyl phosphate coordinated to complex **1** revealed that the mechanism of hydrolysis changes from concerted to a two-step addition−elimination as the coordinated substrate changes from mono- to diester.[16]

In a recent publication, we used LFER and KIE data to assess the transition states and mechanisms for PP1 and hydroxide-catalyzed hydrolysis of aryl methylphosphonates.[10] In this paper we extend these studies to the TACN Co(III)-aryl methylphosphonate complexes **1a**−**e** (Figure 1A; TACN = 1,4,7-triazacyclononane). This establishes a comparative base for phosphonate versus phosphate mechanisms, since the hydrolytic mechanisms of phosphate monoesters and diesters bound to this complex are well established,[14−18] as well as how the mechanism of the CoTACN complex compares to the mechanism of

(8) Kelly, S. J.; Butler, L. G. *Biochem. Biophys. Res. Commun.* **1975**, *66*, 316–321. Kelly, S. J.; Butler, L. G. *Biochemistry* **1977**, *16*, 1102–1104. Kelly, S. J.; Dardinger, D. E.; Butler, L. G. *Biochemistry* **1975**, *14*, 4983–4988.
(9) Hickey, M. E.; Waymack, P. P.; Van Etten, R. L. *Arch. Biochem. Biophys.* **1976**, *172*, 439–448.
(10) McWhirter, C.; Lund, E. A.; Tanifum, E. A.; Feng, G.; Sheikh, Q. I.; Hengge, A. C.; Williams, N. H. *J. Am. Chem. Soc.* **2008**, *130*, 13673–82.
(11) Sträter, N.; Klabunde, T.; Tucker, P.; Witzel, H.; Krebs, B. *Science* **1995**, *268*, 1489–1492.
(12) Goldberg, J.; Huang, H. B.; Kwon, Y. G.; Greengard, P.; Nairn, A. C.; Kuriyan, J. *Nature* **1995**, *376*, 745–753.
(13) Kirby, A. J.; Jencks, W. P. *J. Am. Chem. Soc.* **1965**, *87*, 3209–3216.
(14) Williams, N. H.; Lebuis, A.-M.; Chin, J. *J. Am. Chem. Soc.* **1999**, *121*, 3341–3348.
(15) Williams, N. H.; Cheung, W.; Chin, J. *J. Am. Chem. Soc.* **1998**, *120*, 8079–8087.
(16) Humphry, T.; Forconi, M.; Williams, N. H.; Hengge, A. C. *J. Am. Chem. Soc.* **2004**, *126*, 11864–9.
(17) Humphry, T.; Forconi, M.; Williams, N. H.; Hengge, A. C. *J. Am. Chem. Soc.* **2002**, *124*, 14860–1.
(18) Wahnon, D.; Lebuis, A.-M.; Chin, J. *Angew. Chem., Int. Ed. Engl.* **1995**, *34*, 2412–2414. Williams, N. H.; Takasaki, B.; Wall, M.; Chin, J. *Acc. Chem. Res.* **1999**, *32*, 485–493.

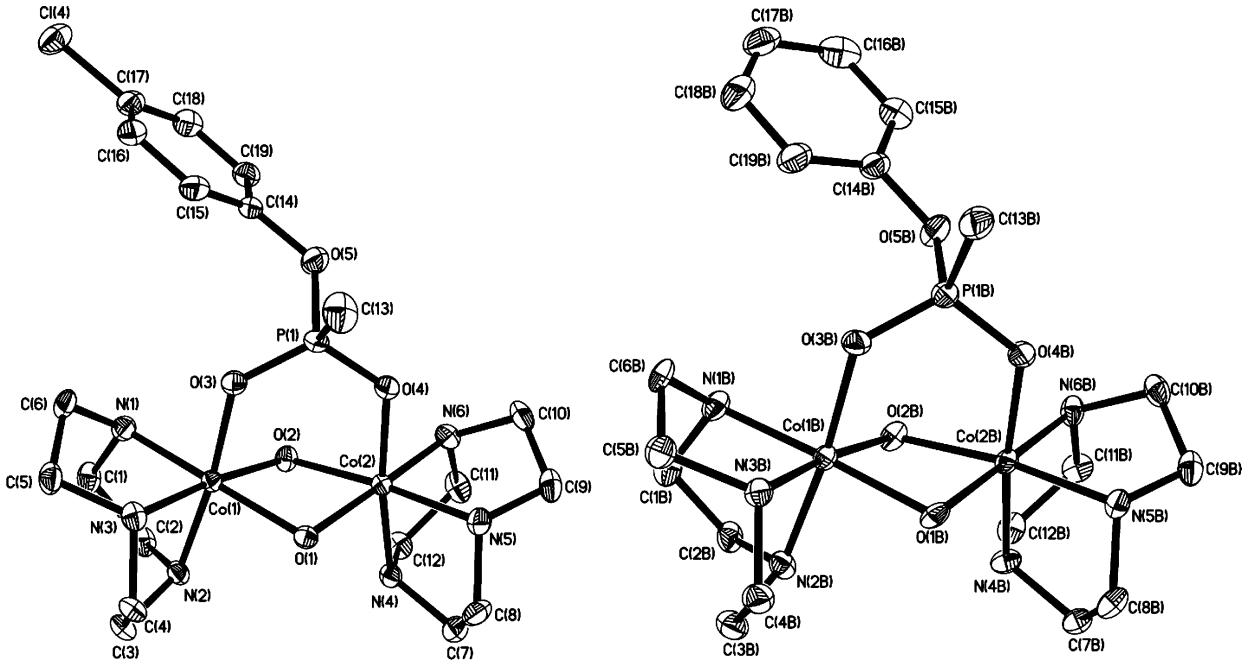

Figure 2. Crystal structures of the cations of **1d** and **1e**.

PP1-catalyzed phosphonate hydrolysis. Linear free energy relationships were obtained by measuring the rate constant for the reactions of a series of aryl methylphosphonates, allowing the measurement of the Brønsted β_{lg} parameter. The activation parameters and kinetic isotope effects were measured for the reaction of the complex of *p*-nitrophenyl methylphosphonate (**1b**; Figure 1B).

Results

The aryl methylphosphonates were synthesized as previously described,[10] and incorporated into the complexes **1a**−**e** as previously described for the related mono- and diester complexes.[14−17] We were able to crystallize complexes **1d** and **1e**, which revealed that the aryl methylphosphonates bridge the two Co(III) ions as previously established with the mono- and diester complexes (Figure 2). In both cases, the Co(III) ions are 2.91 Å apart. For **1d**, the phosphorus atom is equidistant from both bridging hydroxides (3.23 Å), but in **1e**, one hydroxide is within 3.14 Å, and the other within 3.28 Å. Similar symmetric and asymmetric bridging of the two Co(III) ions has been observed with phosphate diester[18] and monoester[15] complexes, suggesting that the phosphate or phosphonate can rock about the two oxygen atoms coordinated to the Co(III) ions with little energetic penalty. For the oxygens coordinated to the Co(III) ions, the PO bond lengths are 1.50 − 1.51 Å, and the bond lengths to the leaving groups are 1.59 Å (**1d**) and 1.61 (**1e**). These are very similar to the bond lengths in an analogous 4-nitrophenylphosphate complex (1.50 and 1.59 Å respectively). This complex is protonated on the remaining oxygen, and so this phosphate is likely to be representative of a diester structure. The remaining bonds show greater differences, with the phosphonates having PC bond lengths of 1.78 (**1d**) and 1.77 Å (**1e**), and the monoester having a POH bond length of 1.54 Å. All these bond lengths are typical of phosphates in the ground state, and so there is no strong evidence for any change in the ground state structure of the phosphonates due to their coordination to the Co(III) ions.

Under the reaction conditions we employed (25 °C, $I = 0.1$ M ($NaClO_4$), 50 mM buffer) the bridging aryl methylphosphonates **1a**−**d** are cleanly hydrolyzed, releasing the substituted phenol and leaving methylphosphonate bound in the complex (**1f**). For complex **1e**, some dissociation of phenyl methylphosphonate from the complex also occurred. Integrating the ^{31}P NMR spectrum of the reaction products from the hydrolysis of **1e** in a buffered solution (50 mM, pH 10.0, 50% D_2O in H_2O) showed the percentage dissociation is only 7%, and so a small correction to the overall observed rate constant was made to generate the observed rate constant for hydrolysis. Similarly, HPLC analysis of all the reaction mixtures for **1e** confirmed that a constant 93:7 ratio of hydrolytic (phenolate) and dissociative (phenyl methylphosphonate) products formed at each pH investigated. Hence, the rate of hydrolysis is much greater than the rate of dissociation for all the complexes **1a**−**1e**. The corresponding first order rate constants can be fitted to eq 1 accurately, showing that all the reactions are specific base catalyzed over the pH range that we have studied (Figure 3) and giving values of $k_h = 3.47 \pm 0.06 \times 10^6$ $M^{-1}s^{-1}$ (**1a**), $4.1 \pm 0.1 \times 10^5$ $M^{-1}s^{-1}$ (**1b**), $3.7 \pm 0.1 \times 10^4$ $M^{-1}s^{-1}$ (**1c**), $8.7 \pm 0.3 \times 10^2$ $M^{-1}s^{-1}$ (**1d**) and $1.57 \pm 0.04 \times 10^2$ $M^{-1}s^{-1}$ (**1e**).

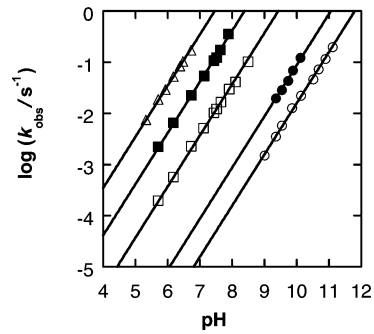

Figure 3. pH-rate profiles for the hydrolysis of complexes **1a**−**e**. The solid lines were fitted by linear least-squares regression to give the β_{lg} parameters reported in the text and in Table 1.

$$k_{obs} = k_h[HO^-] \quad (1)$$

Table 1. KIE Results for Reactions of **1b**, for the PP1 Catalysed Hydrolysis of the Uncomplexed Ester, and for a Monoester and Diester Coordinated to the Same Complex[a]

isotope effect	**1b**	PP1-catalyzed hydrolysis of *p*-nitrophenyl methylphosphonate[10]	*p*-nitrophenyl phosphate complex[16]	*methyl-p*-nitrophenyl phosphate complex[17,19]
^{15}k	1.0014 (1)	1.0010 (1)	1.0011 (4)	1.0026 (2)
$^{18}k_{lg}$	1.0228 (3)	1.0129 (2)	1.019 (1)	1.029 (2)
$^{18}k_{nonbridge}$	0.9954 (1)	0.9973 (5)	na	1.0006 (4)
$^{18}k_{nuc}$	1.011 (2)	na	1.013 (1)	0.934 (2)
β_{lg}	-1.12 ± 0.03	-0.30	-1.10 ± 0.02[14]	-1.38 ± 0.01[15]

[a] Also shown are the Brønsted β_{lg} values for a series of aryl esters.

The hydrolysis of **1b** was measured over the temperature range 20−40 °C to construct an Arrhenius plot, which yielded activation parameters of $\Delta H^{\ddagger} = 40 \pm 1$ kJ mol^{-1} and $\Delta S^{\ddagger} = -2.7 \pm 1$ J mol^{-1} K^{-1}, compared to $\Delta H^{\ddagger} = 70 \pm 1$ kJ mol^{-1} and $\Delta S^{\ddagger} = -103 \pm 1$ J mol^{-1} K^{-1}, for the hydroxide-catalyzed hydrolysis of unbound *p*-nitrophenyl methylphosphonate. The activation parameters for the other aryl methylphosphonates were also measured, and revealed very similar values for $\Delta S^{\ddagger}$ (J mol^{-1} K^{-1}; **1a**: -116 ± 11; **1c**, -111 ± 6; **1d**, -113 ± 4; **1e**, -117 ± 30) but differing values for $\Delta H^{\ddagger}$ (kJ mol^{-1}; **1a**: 62 ± 4; **1c**, 72 ± 2; **1d**, 76 ± 1; **1e**, 78 ± 10).

Figure 1B shows the positions at which KIEs were measured for complex **1b**, at pH 5.7 and 22 °C. Table 1 shows the KIE results, and the Brønsted β_{lg} for the complexes **1a**−**e**. For comparison, data are included for the PP1-catalyzed hydrolysis of aryl methylphosphonates, and for the hydrolysis of complexed phosphate mono- and diesters. The numbers in parentheses indicate the standard errors in the last decimal place. The common notation for isotope effects is used here, which is a leading superscript of the heavier isotope to indicate the isotope effect on the following kinetic quantity; for example ^{15}k denotes k_{14}/k_{15}, the nitrogen-15 isotope effect on the rate constant k.

Discussion

Kinetic isotope effects reflect the difference in bonding to the labeled atom between the ground state and transition state of the rate-limiting step of a chemical reaction.[20] Consequently they serve as a useful tool in probing transition state structures and reaction mechanisms of both catalyzed and uncatalyzed reactions, including phosphoryl transfer. A primary kinetic isotope effect at an atom undergoing bond cleavage will be normal, due to the preference of the heavier isotope for the lower energy (more tightly bonded) position. Secondary kinetic isotope effects are normal (>1) when the labeled atom becomes more loosely bonded in the transition state, or inverse (<1) when bonding becomes tighter. A large number of KIEs has been reported for enzymatic, uncatalyzed, and metal-catalyzed phosphate ester reactions, which provides a background for the interpretation of the KIE data measured in this study.

The magnitude of ^{15}k reflects the amount of negative charge developed on the leaving group in the transition state. It results from delocalization of charge arising from the P−O bond fission, which involves the nitrogen via resonance. This KIE is increasingly normal as more charge is delocalized, reaching an observed maximum of 1.003 for a transition state with extensive leaving group bond fission and no charge neutralization.[21] The $^{18}k_{lg}$ KIE is a measure of the extent of P−O fission in the transition state. A large normal value for this KIE indicates extensive P−O bond weakening in the transition state, and can reach 1.03 for a loose transition state with extensive bond fission.[21] The secondary isotope effect $^{18}k_{nonbridge}$ reveals changes in bonding to the phosphoryl group (metaphosphate-like or phosphorane-like) in the transition state. While bond order considerations may be dominant in primary kinetic isotope effects, bending, torsional and vibrational modes can be more dominant for an atom bonded to a site undergoing a change in hybridization or steric considerations in the transition state. An increase in bond order to bridge atoms would result in an inverse KIE, while a decrease would result in a normal KIE. An increase in steric congestion in the transition state results in "stiffening" of bending modes giving rise to an inverse KIE and vice versa. A recent density functional theory analysis of the uncatalyzed hydrolysis of *p*NPP obtained a loose transition state with computed[22] leaving group and nonbridge KIEs close to the experimental[23] ones. The $^{18}k_{nuc}$ is a measure of nucleophilic participation in the transition. Nucleophile KIEs are generally normal and large for an early transition state and diminishes, as the degree of bond formation increases, to inverse if the bond to the nucleophile is completely formed in the transition state.[24−26] The later is observed when nucleophilic attack results in an intermediate, whose breakdown is rate-limiting.[16,17] Further discussion of nucleophile isotope effects can be found in the Supporting Information.

The Nucleophile. The nucleophile in the hydrolysis of TACN Co(III) complex-bound phosphate esters is an oxo species formed from initial deprotonation of one of the bridging hydroxides (Scheme 1), as demonstrated by the specific base catalysis observed (Figure 3).[14] No evidence for pH independent cleavage is observed, showing that the bridging hydroxide is too poor a nucleophile to promote departure of the leaving group. The X-ray structures show that the bridging oxygen atoms are within van der Waals contact of the phosphorus atom, and in the structure of **1d** one of these atoms is almost collinear with the P−O bond of the leaving group (12° from linearity); the reaction only requires the phosphonate to pivot around the Co(III) coordinated nonbridging oxygens to induce bond formation. Consistent with a structure that requires very little movement to occur to progress from the ground state to the transition state, the entropy of activation of **1b** is very close to

(19) Rawlings, J.; Cleland, W. W.; Hengge, A. C. *J. Am. Chem. Soc.* **2006**, *128*, 17120–5.
(20) Melander, L.; Saunders, W. H. *Reaction Rates of Isotopic Molecules*; Robert E., Ed.; Krieger: Malabar, FL, 1987.
(21) Hengge, A. C. *Acc. Chem. Res.* **2002**, *35*, 105–12.
(22) Zhang, L.; Xie, D.; Xu, D.; Guo, H. *Chem. Commun.* **2007**, 1638–40.
(23) Hengge, A. C.; Edens, W. A.; Elsing, H. *J. Am. Chem. Soc.* **1994**, *116*, 5045–5049.
(24) Cassano, A. G.; Anderson, V. E.; Harris, M. E. *J. Am. Chem. Soc.* **2002**, *124*, 10964–10965.
(25) Cassano, A. G.; Anderson, V. E.; Harris, M. E. *Biochemistry* **2004**, *43*, 10547–10559.
(26) Marlier, J. F. *J. Am. Chem. Soc.* **1993**, *115*, 5953–5956. Marlier, J. F.; Dopke, N. C.; Johnstone, K. R.; Wirdzig, T. J. *J. Am. Chem. Soc.* **1999**, *121*, 4356–4363. Paneth, P.; O'Leary, M. H. *J. Am. Chem. Soc.* **1991**, *113*, 1691–1693. Westaway, K. C.; Fang, Y.; Persson, J.; Matsson, O. *J. Am. Chem. Soc.* **1998**, *120*, 3340–3344.

Scheme 1. Proposed Mechanism and Transition State Structure

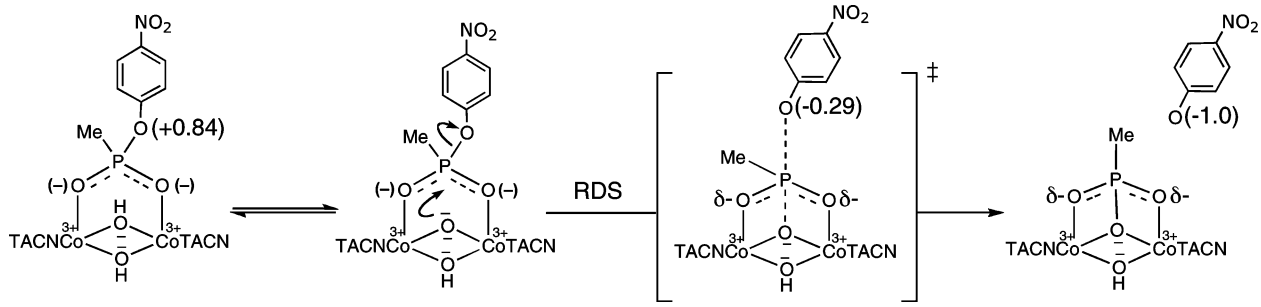

zero (-3 J mol^{-1} K^{-1}), in contrast to the intermolecular reaction between the uncomplexed phosphonate and hydroxide that has a value (-103 J mol^{-1} K^{-1}) typical of a bimolecular reaction.

The labeled complex used for the determination of the nucleophile isotope effect has an ^{18}O label at both of the bridging positions (see Figure 1). In our analysis, we assume that the KIE arises from the nucleophilic atom, and that the second oxygen contributes negligibly to the observed isotope effect. The normal $^{18}k_{nuc}$ value of 1.011 ± 0.002 for complex **1b** indicates the presence of nucleophilic participation in the rate-limiting step. This value reflects the fractionation of isotopes on the equilibrium deprotonation of the bridging hydroxide to form the oxo nucleophile, as well as the kinetic isotope effect on nucleophilic attack. The equilibrium isotope effect (EIE) for deprotonation of hydroxide to yield a metal-bound oxide, either singly or doubly coordinated to metal ions, has not been reported. The EIE for deprotonation of a water molecule coordinated to a single Co(III) ion is 1.012, obtained from the EIEs between $(NH_3)_5$Co(III)$-OH_2$ and water (1.0196) and $(NH_3)_5$Co(III)$-$OH and water (1.008).[27] Coordination to a second Co(III) should further reduce the EIE. This trend arises from the fact that the force constant for the coordination of oxygen to the metal ions will be greater for hydroxide than for water, and in turn, greater for the oxide than for hydroxide. Thus, the fractionation arising from loss of the O$-$H bond is partly compensated for by enhanced coordination to the Co(III) ions. As a result, the EIE for deprotonation in this reaction should be smaller than the observed $^{18}k_{nuc}$ of 1.0105 ± 0.0005. If so, this implies that the KIE on nucleophilic attack is small and normal, an indication of nucleophilic bond formation in the rate-limiting step. This assumption is further supported by an earlier observation by Cassano et al. that the $^{18}k_{nuc}$ for the hydrolysis of a diester substrate changes from 1.068 ± 0.007 for free hydroxide catalyzed hydrolysis[24] to 1.027 ± 0.013 for Mg^{2+}-hydroxide coordinated hydrolysis.[25] This difference was also attributed to a reduction in the fractionation factor for nucleophile deprotonation arising from coordination to magnesium ion.

The Leaving Group. Complementing KIE data, Brønsted β values provide information on the changes occurring at an atom if it is electronically varied in a series of kinetic or equilibrium experiments. The impact of varying the pK_a of the leaving group will depend on the degree of bonding to the leaving atom in the transition state, but also on its solvation and electronic environment, so does not provide a simple measure of bond order. If the equilibrium effect of the perturbation (e.g., leaving group variation) is known, the kinetic effect can be normalized to provide a measure of the position of the transition state in terms of effective charge at the leaving atom.[28]

(27) Hunt, H. R.; Taube, H. *J. Phys. Chem.* **1959**, *63*, 124–125.

For the bound phosphonates, the Brønsted plot (Figure 4) reveals that $\beta_{lg} = -1.12 \pm 0.03$ for hydroxide catalyzed hydrolysis of the phosphonates coordinated to the Co(III) complex. If we assume that the effective charge on the phenolic oxygen of bound aryl methylphosphonate is about the same as that in a doubly protonated (neutral) aryl phosphate, we can normalize the Brønsted data. The amount of charge on the phenolic oxygen in phenolate anion and in doubly protonated aryl phosphate are reported as -1, and $+0.83$, respectively.[28] The total change in the charge on hydrolysis is thus estimated to be $-1 - 0.83 = -1.83$. Since the value of β_{lg} is -1.12, the extent of P$-$O bond cleavage at the transition state for the reactions is estimated to be about 1.12/1.83 = 0.61 and the effective charge on the phenolic oxygen at the transition state is expected to be about $0.83 - 1.12 = -0.29$.[29] By way of comparison, the same analysis for the uncomplexed phosphonates gives $\beta_{lg} = -0.69 \pm 0.02$ (close to the value of -0.64 ± 0.03 reported for hydrolysis of an analogous group of methoxy aryl diesters under the same reaction conditions,[15] suggesting a later transition state for the more reactive complexed species. If we assume that the uncomplexed phosphonate has a starting effective charge that is similar to the isoelectronic monoprotonated aryl phosphate (+0.74), then the extent of cleavage can be estimated as 0.69/1.74 = 0.40 and the effective charge on the phenolic oxygen at the transition state is about $0.74 - 0.69 = +0.05$.

These analyses use the assumption that a neutral OH or Me substituent on the transferring phosphorus will have a similar effect on the β_{eq} value, but it is likely that the effect of changing an oxygen to a carbon substituent will be to reduce the β_{eq} value for hydrolysis as the less electronegative methyl group moderates the electrophilicity of the phosphorus center. For example, β_{eq} decreases from 1.87 for diethylphosphate transfer to 1.30 for diphenylphosphate transfer to 1.22 for diphenylphosphinate

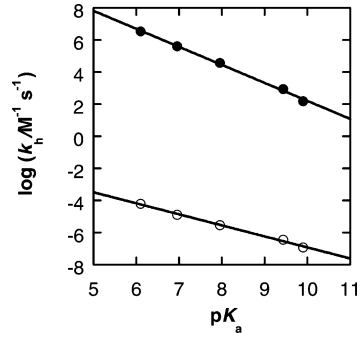

Figure 4. Linear free energy relationship between leaving group pK_a and second-order rate constant for hydroxide catalyzed hydrolysis of **1a**$-$**e** (●, $\beta_{lg} = -1.12 \pm 0.03$; intercept = 13.4 ± 0.3) and corresponding aryl methyl phosphonates (○, $\beta_{lg} = -0.69 \pm 0.02$; intercept = -0.1 ± 0.2). The solid lines were fitted by linear least-squares regression.

transfer.[30] This would suggest that the transition states are more advanced than indicated above. If the value for β_{eq} is reduced to an estimate of 1.3, the extent of reaction for the complexed and uncomplexed phosphonates would be 0.86 and 0.53 respectively. By way of further comparison, the overall picture is of a synchronous transition state for the uncomplexed phosphonate with little charge development at the leaving oxygen atom, but a rather more advanced transition state for the complexed phosphonate with more substantial charge development.

The estimate of leaving group departure in the transition state from LFER analysis of the phosphonate complexes is in reasonable agreement with both the $^{18}k_{lg}$ and the ^{15}k for **1b**. The primary $^{18}k_{lg}$ of 1.0228 is 2/3 of 1.0340, the largest magnitude that has been observed for this isotope effect with the *p*-nitrophenyl leaving group.[31] The magnitude of ^{15}k, 1.0014, is about one-half of its maximum of 1.0030,[21] indicating about a half of a formal negative charge on the leaving group. This is reasonable agreement given the small magnitude of this secondary KIE. Also,^{15}k is sensitive only to the extent of charge delocalization, which will be affected by the neighboring negative charge on the phosphoryl group in the transition state. The maximal values of ^{15}k have been observed in reactions of the *p*NPP dianion, in which charge repulsion between the proximal anionic phosphoryl group and the leaving group enhances delocalization. In the present complex, coordination may lessen the negative charge on the phosphoryl, and hence its effect on delocalization.

Interestingly, the LFER and KIE data for the phosphate diester complex differ significantly from those of the phosphonate complex **1b** despite the isoelectronic nature of the diester and the methylphosphonate. The data for the diester complex, particularly the inverse $^{18}k_{nuc}$, are more consistent with a two-step addition−elimination mechanism with rate-limiting expulsion of the leaving group despite the low basicity of nitrophenolate; this unusual outcome may result from strain associated with formation of a coordinated phosphorane intermediate.[16] In acidic solution, diphenyl methylphosphonate incorporates isotopically labeled water at about 8% the rate of hydrolysis,[32] implicating a stable phosphorane intermediate, whereas neutral phosphate esters such as triphenyl phosphate do not show any observable incorporation of solvent label into the starting ester, and incorporation is concomitant with hydrolysis.[33] These observations would suggest that the substitution of a methoxy with a methyl group would favor the associative pathway, so it is not clear why the methylphosphonate should not also form a phosphorane intermediate when constrained in the context of the Co(III) complex.

A combination of the normal $^{18}k_{nuc}$ and a significantly large normal $^{18}k_{lg}$ indicate that both bond formation and bond fission occur in the rate-limiting step, consistent with a concerted mechanism. The similarity of the LFER and KIE data for complex **1b** with the corresponding data for the phosphate monoester complex make evident a similar transition state for the two reactions.

This implies that when bound to the dinuclear metal center, the phosphonate ester reacts more like a phosphate monoester than the diester for which it is assumed as an analogue. It is interesting to note that a similar observation is apparent when examining the effect that catalysis by PP1 has on phosphate monoester and methylphosphonate ester hydrolysis. It appears that the dinuclear metal ion reaction center stabilizes transition states that are altered from their uncomplexed counterparts to present very similar kinetic parameters for both phosphate monoesters and methylphosphonate esters. A distinction with the PP1 catalyzed reaction lies in the observation that a much higher sensitivity to the leaving group is observed for the TACN Co(III) complexes for both substrates. However, it is likely that the enzyme utilizes general acid catalysis at the leaving group as part of its catalytic machinery, which would suppress this sensitivity, whereas in the model complex no additional functionality is available. With similar effective charges at the leaving group in the transition state, it could be expected that such interactions will have a similar effect on both reactants. A second contrast is that the model complexes show ∼1000-fold higher reactivity when the methylphosphonate is bound compared to the phosphate monoester, whereas in the PP1 reactions, the monoesters are ∼10-fold more reactive. However, the PP1 parameters also include substrate binding from solution, whereas the complexes are analogous to the Michaelis complex. The higher charge of the monoester dianion would suggest that enhanced ground state binding would be expected, offsetting potential differences in intrinsic reactivity when bound. We also note that the methylphosphonate complexes are about 10-fold more reactive than the corresponding aryl methyl phosphate diesters, which reflects the differences also observed in the PP1 catalyzed reactions of these substrates. Here, the ground state binding may be expected to be less of a differential factor and so may represent subtle differences in the stabilization of the two functional groups. This difference is matched by the differential in reactivity of the uncomplexed substrates, where the diester is also about 10-fold less reactive than the methylphosphonate.

The small inverse $^{18}k_{nonbridge}$ KIE, 0.9954 ± 0.0001, implies little change in bond order to the nonbridge oxygen atoms. This is not inconsistent with the concerted mechanism implied by the other data. The interpretation of $^{18}k_{nonbridge}$ is difficult due to multiple contributions; not only differences in P−O bond order, but accompanying changes in the interactions between these oxygen atoms and the Co atoms will also contribute. The trigonal bipyramidal transition state will also result in changes in the bending modes of the latter bonds. In uncatalyzed reactions, the loose, metaphosphate-like transition states of monoester reactions result in very small, inverse $^{18}k_{nonbridge}$ values, while the more symmetric transition states in diester reactions give rise to small, normal values, which become still larger in the more associative reactions of triesters. A concerted reaction with synchronous bond formation and bond fission should result in minimal bond order changes between phosphorus and the nonbridge oxygen atoms, but in a reaction involving a metal complex, the bending modes may well stiffen resulting in an inverse effect. For comparison, the hydrolysis of the complex of the diester ethyl *p*-nitrophenyl phosphate is accompanied by a small normal $^{18}k_{nonbridge}$ of 1.0006 ± 0.0004.[19] The analogous KIE for the phosphate monoester complex cannot

(28) Williams, A. *Free Energy Relationships*; Royal Society of Chemistry: Cambridge, UK, 2003.
(29) Williams, A. *Adv. Phys. Org. Chem.* **1992**, *27*, 1–55.
(30) Ba-Saif, S. A.; Waring, M. A.; Williams, A. *J. Chem. Soc., Perkin Trans. 2* **1991**, 1653–1659.
(31) Hoff, R. H.; Wu, L.; Zhou, B.; Zhang, Z.-Y.; Hengge, A. C. *J. Am. Chem. Soc.* **1999**, *121*, 9514–9521.
(32) Sigal, I.; Westheimer, F. H. *J. Am. Chem. Soc.* **1979**, *101*, 752–754.
(33) Bunton, C. A.; Farber, S. J. *J. Org. Chem.* **1969**, *34*, 3396–3403.

be measured due to nonequivalence of the three nonbridging oxygens in the complex.

Conclusions

The complexes **1a**−**e**, are very efficiently hydrolyzed, with a rate acceleration of ~10^{10}-fold compared to the uncomplexed methylphosphonate reacting with hydroxide. This acceleration is accompanied by a change in transition state structure that involves greater bond cleavage and effective charge development at the leaving oxygen. Unlike the analogous complexes incorporating phosphate diesters, a mechanistic change is not observed. As with the PP1 catalyzed reactions of phosphate monoester and methylphosphonate substrates, there are close similarities in the characteristics of **1a**−**e** and the analogous phosphate monoester complexes. The transition states for hydrolysis of complexed aryl methylphosphonates and aryl phosphates are much more similar to one another than are the hydrolysis reactions of the uncomplexed substrates.

Experimental Methods

Synthesis of Complexes 1a−**e.** All complexes were prepared from their respective aryl phosphonate salts[6] using the following general procedure: [(1,4,7-Triazacyclononane)$_2$Co$_2$(OH)$_3$](ClO4)$_3$ (36.3 mg, 0.05 mmol), prepared as previously reported,[8] was mixed with one mole equivalent of aryl methylphosphonate and 0.5 mL of 0.1 M perchloric acid. The mixture was warmed gently to give a clear red-purple solution and allowed to cool slowly. The product complex was precipitated by adding solid sodium perchlorate and recrystallized from 0.01 M perchloric acid to obtain a purple solid. The yields ranged between 53−75%.

***p*-Nitro-*m*-fluorophenyl Methylphosphonate-TACN-Co(III) Complex (1a).** ^{1}H NMR (250 MHz, D_2O, 0.01 M $HClO_4$) δ/ppm 8.22 (m, 1H, Ar−H), 7.16−7.26 (m, 2H, Ar−H), 6.76 (br s, 2H, 2NH), 6.60 (br s, 2H, 2NH), 6.45 (br s, 2H, 2NH), 3.20−3.30 (m, 12H, CH_2N), 2.50−2.71 (m, 12H, CH_2N), 1.67 (d, J = 17.40 Hz, 3H, CH_3); ^{31}P NMR (103.3 MHz, D_2O, 0.01 M $HClO_4$) δ/ppm 50.75; MS (TOF MS EI+), *m/z*, 703 (6%), 567(98%), 283 (100%). Anal. calcd for $C_{19}H_{38}Cl_3Co_2FN_7O_{19}P.H_2O$:C, 23.75; H, 4.20; N, 10.21. Found: C, 23.76; H, 4.36; N, 10.06.

***p*-Nitrophenyl Methylphosphonate-TACN-Co(III) Complex (1b).** ^{1}H NMR (250 MHz, D_2O, 0.01 M $HClO_4$) δ/ppm 8.31 (d, J = 9.16 Hz, 2H, Ar−H), 7.37 (d, J = 9.16 Hz, 2H, Ar−H), 6.74 (br s, 2H, 2NH), 6.60 (br s, 2H, 2NH), 6.44 (br s, 2H, 2NH), 3.20−3.30 (m, 12H, CH_2N), 2.50−2.72 (m, 12H, CH_2N), 1.66 (d, J = 17.09 Hz, 3H, CH_3); ^{31}P NMR (103.3 MHz, D_2O, 0.01 M $HClO_4$) δ/ppm 50.64; MS (TOF MS EI+), *m/z*, 824 (M − ClO_4^-, 100%), 825 (24%), 826 (70%), 827 (16%), 828 (14%), 829 (3%); HR-MS (TOF MS EI+) calculated for $C_{19}H_{39}N_7O_{15}PCl_2Co_2$ (M − ClO_4^-): 824.0283, found: 824.0284.

***m*-Nitrophenyl Methylphosphonate-TACN-Co(III) Complex (1c).** ^{1}H NMR (250 MHz, D_2O, 0.01 M $HClO_4$) δ/ppm 8.12 (s, 1H, Ar−H), 8.07−8.09 (m, 1H, Ar−H), 7.55−7.68 (m, 2H, Ar−H), 6.74 (br s, 2H, 2NH), 6.62 (br s, 2H, 2NH), 6.44 (br s, 2H, 2NH), 3.17−3.30 (m, 12H, CH_2N), 2.60−2.72 (m, 12H, CH_2N), 1.59 (d, J = 17.39 Hz, 3H, CH_3); ^{31}P NMR (103.3 MHz, D_2O, 0.01 M $HClO_4$) δ/ppm 51.24; MS (TOF MS EI+), *m/z*, 824 (M - ClO_4^-, 30%), 826 (15%), 625 (32%), 627 (17%), 404 (100%), 402 (48%); HR-MS (TOF MS EI+) calculated for $C_{19}H_{39}N_7O_{15}PCl_2Co_2$ (M − ClO_4^-): 824.0283, found: 824.0250.

***p*-Chlorophenyl Methylphosphonate-TACN-Co(III) Complex (1d).** ^{1}H NMR (250 MHz, D_2O, 0.01 M $HClO_4$) δ/ppm 7.42 (d, J = 8.85 Hz, 2H, Ar−H), 7.16 (d, J = 8.85 Hz, 2H, Ar−H), 6.69 (br s, 2H, 2NH), 6.51 (br s, 2H, 2NH), 6.42 (br s, 2H, 2NH), 3.20−3.30 (m, 12H, CH_2N), 2.50−2.70 (m, 12H, CH_2N), 1.67 (d, J = 17.39 Hz, 3H, CH_3); ^{31}P NMR (103.3 MHz, D_2O, 0.01 M $HClO_4$) δ/ppm 50.85; MS (TOF MS EI+), *m/z*, 813 (M - ClO_4^-, 5%), 815 (5%), 307 (100%); HR-MS (TOF MS EI+) calculated for $C_{19}H_{39}N_6O_{13}PCl_3Co_2$ (M − ClO_4^-): 813.0042, found: 813.0004.

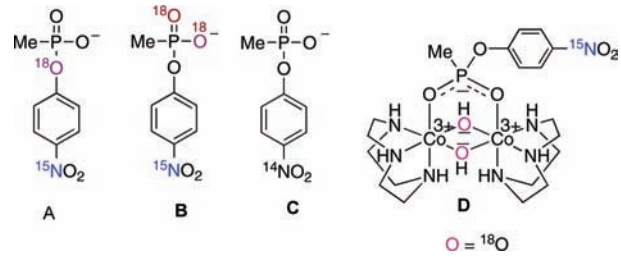

Figure 5. Isotopic isomers of *p*-nitrophenyl methylphosphonate used for isotope effects measurements.

Phenyl Methylphosphonate-TACN-Co(III) Complex (1e). ^{1}H NMR (250 MHz, D_2O, 0.01 M $HClO_4$) δ/ppm 7.41−7.48 (m, 2H, Ar−H), 7.18−7.30 (m, 3H, Ar−H), 6.68 (br s, 2H, 2NH), 6.43 (br s, 4H, 2NH), 3.17−3.25 (m, 12H, CH_2N), 2.50−2.74 (m, 12H, CH_2N), 1.58 (d, J = 17.09 Hz, 3H, CH_3); ^{31}P NMR (103.3 MHz, D_2O, 0.01 M $HClO_4$) δ/ppm 50.78; MS (TOF MS EI+), *m/z*, 779 (M − ClO_4^-, 20%), 780 (5%), 781 (14%), 782 (3%), 625 (25%), 589 (17%), 359 (100%); HR-MS (TOF MS EI+) calculated for $C_{19}H_{40}N_6O_{13}PCl_2Co_2$ (M − ClO_4^-): 779.0432, found: 779.0444.

Synthesis of Isotopically Labeled Compounds and Complexes (Figure 5). Natural abundance *p*-nitrophenyl methylphosphonate, [^{14}N]-*p*-nitrophenyl methylphosphonate (C), [^{15}N]-*p*-nitrophenyl methylphosphonate, [^{15}N]-*p*-nitrophen[^{18}O]yl methylphosphonate (A) and [^{15}N]-*p*-nitrophenyl methyl-[$^{18}O_2$]-phosphonate (B) were synthesized as previously described.[10] The nitrogen isotope effect ^{15}k was measured using natural abundance complex **1b**. For measurement of $^{18}k_{lg}$ the complex was prepared from a mixture of A and C, reconstituted to near the natural abundance of ^{15}N; similarly, $^{18}k_{nonbridge}$ was measured using a complexed mixture of B and C.

The nucleophile ^{18}O isotope effect ($^{18}k_{nuc}$) was measured using a mixture of the complex **1b** prepared from [^{14}N]-*p*-nitrophenyl methylphosphonate with natural abundance oxygen at the bridging hydroxide positions, with that prepared from [^{15}N]-*p*-nitrophenyl methylphosphonate with ^{18}O at the bridging hydroxide positions (D). The ^{18}O was incorporated as previously described[17] and 93 ± 1% of the product was found to possess the isotopic label at both bridging positions, using electrospray mass spectrometry.

Kinetics. The hydrolysis of aryl methylphosphonate-TACN-Co(III) complexes (**1a**−**e**) were followed at 25 °C in aqueous solution with 50 mM buffer and I = 0.1 M ($NaClO_4$). pHs were measured before and after each reaction, and did not change. Buffers used were 2-(*N*-morpholino)ethanesulfonic acid (MES, pH 5.5−6.7), 4-(2-hydroxyethyl)-1-piperazine-ethanesulfonic acid (HEPES, pH 6.8−8.0), 4-(2-hydroxyethyl)-1-piperazinepropanesulfonic acid (EPPS, pH 7.5−8.7), 2-(*N*-cyclohexylamino)ethanesulfonic acid (CHES, pH 8.6−10.0) and 3-(cyclohexylamino)-1-propanesulfonic acid (CAPS, pH 9.7−10.5). In a typical experiment, the reactions was initiated by injection of 4.5 μL of a stock solution of **1a**−**e** (10 mM in 0.01 M HClO4) into 0.90 mL of 50 mM buffer solutions at 25 °C (equilibrated in the thermostatted compartment of the spectrophotometer). Formation of substituted phenolate anion was monitored by following the UV−vis absorption change (phenolate, 280 nm; *p*-chlorophenolate, 298 nm; *m*-nitrophenolate, 390 nm; *p*-nitrophenolate, 400 nm; *m*-fluoro-*p*-nitrophenolate, 388 nm). All the reactions were monitored for at least 3 half-lives, and first-order rate constant k_{obsd} were determined by fitting the absorbance change to a first-order exponential curve fit. Accurate first-order kinetics was observed over at least 3 half-lives in all cases. The pK_a of the leaving group phenols under the same experimental conditions were reported before and are used here: phenol, 9.95; *p*-chlorophenol, 9.43; *m*-chlorophenol, 9.00; *m*-nitrophenol, 7.95; *p*-nitrophenol, 6.95; *m*-fluoro-*p*-nitrophenol, 6.10.

Product Analysis. The product of aryl methylphosphonate-TACN-Co(III) complex (**1a**-**e**) hydrolysis was identified by HPLC and ^{31}P NMR. Released phenol was identified by HPLC analysis (Column: Gemini 5u C18 110A 150 × 4.6 mm 5 μm; Eluent: Ammonium phosphate buffer (20 mM, pH 5.3):methanol 60:40) and comparison with authentic samples. ^{31}P NMR analysis reveals that aryl methylphosphonate-TACN-Co(III) complex (5−10 mM), react in a buffered solution (50 mM, pH 10.0, 50% D_2O in H_2O) at 25 °C, to give methyl phosphonate-TACN-Co(III) complex (43.76 ppm). Methyl phosphonate-TACN-Co(III) complex (**1f**) was identified as follows: methanephosphonic acid was used to replace methyl arylphenylphosphonate in the synthesis described above give a purple solid. ^{1}H NMR (250 MHz, D_2O, 0.01 M $HClO_4$) δ/ppm 6.56 (br s, 2H, 2NH), 6.48 (br s, 2H, 2NH), 6.30 (br s, 2H, 2NH), 3.10−3.26 (m, 12H, CH_2N), 2.50−2.75 (m, 12H, CH_2N), 1.49 (d, J = 17.40 Hz, 3H, CH3); ^{31}P NMR (103.3 MHz, 50 mM buffer solution, pH 10.0, 50% D_2O in H_2O) δ/ppm 43.76. [δ 50.15 ppm if using 0.01 M $HClO_4$ in D_2O as solvent]. Phenyl methyl phosphonate-TACN-Co(III) complex (**1e**) reacted to give phenol and methyl phosphonate-TACN-Co complex (**1f**) and also methyl phenyl phosphonate (identified through HPLC and ^{31}P NMR); the percentage hydrolysis is 93.5% under this condition, as measured by integrating the ^{31}P NMR signals.

Kinetic Isotope Effect Experiments. KIE experiments for **1b** were carried out using the competitive method, in which the complex was prepared using labeled phosphonates consisting of an isotopic mixture at the position of interest. The complexes, once formed, do not equilibrate between bound and unbound forms. Therefore the KIEs are those for the nucleophilic reaction and do not have contributions from equilibrium fractionations. The oxygen KIEs were obtained using the nitrogen atom in nitrophenol as a reporter; hence, any reaction processes following release of the leaving group do not affect the isotope effect.

The KIE experiments were carried out in triplicate at room temperature and reaction progress monitored spectrophotometrically at 400 nm. The cobalt-phosphonate complex (85 − 90 mg) was first dissolved in 0.01 N $HClO_4$ (6 mL), in which it is stable. To initiate reaction this solution was injected into 39 mL of 50 mM MES buffer, pH 5.74, resulting in a reaction pH of 5.70. The reaction was allowed to run for approximately one-half-life (∼5 min), then swiftly stopped by adding 0.1 N $HClO_4$ (5 mL) to take the pH to below 2.0.

At this point, one 100 μL aliquot of the reaction mixture was added to a cuvette containing 3 mL of 0.1 N NaOH and the absorbance measured at 400 nm. This results in rapid hydrolysis of remaining complex; the measured absorbance served as the total hydrolysis reference. The product nitrophenol from the reaction mixture was then recovered by extracting the mixture three times with equal volumes of ether. The ensuing aqueous phase which contains the residual (unreacted) complex was assayed by transferring 100 μL to 3 mL 0.1 N NaOH and measuring the absorbance. The ratio of this absorbance to the former gives the fraction of unreacted complex remaining when the reaction was stopped. Subtraction of this value from unity gave the fractional progress of the reaction when it was stopped.

The pH of the solution containing the residual complex was then raised to 7.0 and stirred for ten minutes (∼20 half-lives at this pH), after which it was titrated to pH 4.0 and the liberated *p*-nitrophenol extracted as described above. The ether extractions were separately dried over $MgSO_4$, filtered, and the solvent removed *in vacuo*. The resulting *p*-nitrophenol samples were sublimed under vacuum at 90 °C, and the ^{15}N/^{14}N ratios were measured by isotope ratio mass spectrometry at the University of California, Davis, Stable Isotope Facility.

Activation Parameters. The Arrhenius parameters for **1b** were obtained by measuring the observed rate constants at 20, 25, 30, 35, and 40 °C at three pHs between ∼6 and ∼7 (pH of each solution measured at each temperature). The value of k_h was calculated from each of these profiles using the appropriate value of K_w. The data was plotted as log k_h against 1/T and fitted to the equation log k_h = log A − (E_a/2.303RT) where R = 8.314 J K^{-1}mol^{-1}. Linear least-squares regression gave the Arrhenius parameters log A = 13.1 ± 0.2 and E_a = 42.4 ± 1 kJmol^{-1}. These were converted to the activation parameters at 25 °C by applying the equations $\Delta H^{\ddagger} = E_a - RT$ and $\Delta S^{\ddagger} = R \ln A - R \ln(k\mathrm{Te}/\hbar) = R \ln A - 253.2$ J mol^{-1} K^{-1} (k is the Boltzmann constant and $\hbar$ is Planck's constant). For *p*-nitrophenyl methylphosphonate the observed rate constants were measured at 25, 37, 42, 50, and 60 °C in 0.1 M NaOH and divided by 0.1 to give k_h (having established that the rate of reaction is first order in both substrate and hydroxide at 25 °C). The data was treated as described for **1b** to obtain the Arrhenius parameters logA = 7.82 ± 0.05 and E_a = 72.6 ± 0.4 kJmol^{-1}. A similar procedure was used with compounds **1a** (25−60 °C), **1c** (50−90 °C), **1d** (60−90 °C) and **1e** (70−90 °C) to obtain the values for k_h at 25 °C and the corresponding Arrhenius parameters (logA: **1a**:7.1 ± 0.6; **1c**: 7.4 ± 0.3; **1d**: 7.3 ± 0.2; **1e**: 7.1 ± 1.4. E_a (kJ mol^{-1}): **1a**: 64 ± 4; **1c**: 74 ± 2; **1d**: 79 ± 1; **1e**: 80 ± 10.)

X-Ray Data. Data collected were measured on a Bruker Smart CCD area detector with Oxford Cryosystems low temperature system. Complex scattering factors were taken from the program package SHELXTL[34] as implemented on the Viglen Pentium computer.

Crystal data for **1d**: $C_{19}H_{41}Cl_4Co_2N_6O_{18}P$; M = 932.21; crystallizes from water as purple blocks; crystal dimensions 0.28 × 0.18 × 0.12 mm. Triclinic, a = 9.6420(10), b = 12.0145(13), c = 15.1903(16) Å, α = 86.042(2)°, β = 83.851(2)° γ = 74.685(2)°, U = 1685.9(35) Å^3, Z = 2, D_c = 1.836 Mg/m^3, space group P, Mo Kα radiation (= 0.71073 Å), μ(Mo Kα) = 1.434 mm^{-1}, F(000) = 956. Cell parameters were refined from the setting angles of 2160 reflections (θ range 1.35 < 27.59°). Reflections were measured from a hemisphere of data collected of frames each covering 0.3 degrees in omega. Of the 19590 reflections measured, all of which were corrected for Lorentz and polarization effects and for absorption by semi empirical methods based on symmetry-equivalent and repeated reflections (minimum and maximum transmission coefficients 0.6896 and 0.8467), 5543 independent reflections exceeded the significance level $|F|/\sigma(|F|) > 4.0$. The structure was solved by direct methods and refined by full matrix least-squares methods on F^2. Hydrogen atoms were placed geometrically and refined with a riding model (including torsional freedom for methyl groups) and with U_{iso} constrained to be 1.2 (1.5 for methyl groups) times U_{eq} of the carrier atom. Refinement converged at a final R = 0.0509 (wR_2 = 0.1515, for all 7602 data, 446 parameters, mean and maximum δ/σ) with allowance for the thermal anisotropy of all non-hydrogen atoms. Minimum and maximum final electron density −1.186 and 1.696 e.Å^{-3}. A weighting scheme $w = 1/[\sigma^2(F_o^2) + (0.0833 \times P)^2 + 0.0401 \times P]$ where $P = (F_o^2 + 2 \times F_c^2)/3$ was used in the latter stages of refinement.

Crystal data for **1e**: $C_{38}H_{82}Cl_6Co_4N_{12}O_{35}P_2$; M = 1777.52; crystallizes from water as purple blocks; crystal dimensions 0.301 × 0.18 × 0.12 mm. Triclinic, a = 10.3104(8), b = 18.2269(16), c = 19.6351(17) Å, α = 69.550(3)°, β = 76.632(3)° γ = 73.969(2)°, U = 3285.6(5) Å^3, Z = 2, D_c = 1.797 Mg/m^3, space group P, Mo Kα radiation (= 0.71073 Å), μ(Mo Kα) = 1.387 mm^{-1}, F(000) = 1828. Cell parameters were refined from the setting angles of 1954 reflections (θ range 1.22 < 27.22°). Reflections were measured from a hemisphere of data collected of frames each covering 0.3 degrees in omega. Of the 37547 reflections measured, all of which were corrected for Lorentz and polarization effects and for absorption by semi empirical methods based on symmetry-equivalent and repeated reflections (minimum and maximum transmission coefficients 0.6810 and 0.8512), 7960 independent reflections exceeded the significance level $|F|/\sigma(|F|) > 4.0$. The structure was solved by direct methods and refined by full matrix least-squares methods

(34) Bruker-AXS, LTD. SHELXTL, An integrated system for solving and refining crystal structures from diffraction data (Revision 5.1).

on F^2. Hydrogen atoms were placed geometrically and refined with a riding model (including torsional freedom for methyl groups) and with U_{iso} constrained to be 1.2 (1.5 for methyl groups) times U_{eq} of the carrier atom with the exception of the hydrogens on the water molecules, which were not calculated. Refinement converged at a final $R = 0.0503$ (w$R_2 = 0.1370$, for all 14716 data, 876 parameters, mean and maximum δ/σ) with allowance for the thermal anisotropy of all non-hydrogen atoms. Minimum and maximum final electron density -0.715 and 0.995 e.Å^{-3}. A weighting scheme $w = 1/[\sigma^2(F_o^2) + (0.0681 \times P)^2 + 0.00 \times P]$ where $P = (F_o^2 + 2 \times F_c^2)/3$ was used in the latter stages of refinement.

Acknowledgment. This work was supported by a grant from the National Institutes of Health to ACH (GM47297) and by a grant from the Biology and Biotechnology Science Research Council to NHW (C18734).

Supporting Information Available: Data analysis for calculation of kinetic isotope effects from isotope ratio data and levels of isotopic incorporation into labeled substrates, kinetic data for construction of Arrhenius plot for complex **1b**, kinetic data for complexes **1a**−**e**, LFER plot for complexes **1a-e,** and cif files for complexes **1d** and **1e**. This material is available free of charge via the Internet at http://pubs.acs.org.

JA904134N